



1 **Reconstruction of daily gridded snow water equivalent product for the** 2 **Pan-Arctic region based on a ridge regression machine learning** 3 **approach**

4 Donghang Shao^{1,2}, Hongyi Li^{1,2}, Jian Wang^{1,2}, Xiaohua Hao^{1,2}, Tao Che^{1,2} and Wenzheng Ji^{1,2}

5 ¹Northwest Institute of Eco-Environment and Resources, Chinese Academy of Sciences, Lanzhou, 730000, China

6 ²Heihe Remote Sensing Experimental Research Station, Key Laboratory of Remote Sensing of Gansu Province, Chinese
7 Academy of Sciences, Lanzhou, 730000, China

8 *Correspondence to:* Hongyi Li (lihongyi@lzb.ac.cn)

9 **Abstract.** Snow water equivalent is an important parameter of the surface hydrological and climate systems, and it has a
10 profound impact on Arctic amplification and climate change. However, there are great differences among existing snow water
11 equivalent products. In the Pan-Arctic region, the existing snow water equivalent products are limited time span and limited
12 spatial coverage, and the spatial resolution is coarse, which greatly limits the application of snow water equivalent data in
13 cryosphere change and climate change studies. In this study, utilizing the ridge regression model (RRM) of a machine learning
14 algorithm, we integrated various existing snow water equivalent (SWE) products to generate a spatiotemporally seamless and
15 high-precision RRM SWE product. The results show that it is feasible to utilize a ridge regression model based on a machine
16 learning algorithm to prepare snow water equivalent products on a global scale. We evaluated the accuracy of the RRM SWE
17 product using Global Historical Climatology Network (GHCN) data and Russian snow survey data. The MAE, RMSE, R, and
18 R² between the RRM SWE products and observed snow water equivalents are 0.24, 30.29 mm, 0.87, and 0.76, respectively.
19 The accuracy of the RRM SWE dataset is improved by 24%, 25%, 32%, 7%, and 10% compared with the original AMSR-
20 E/AMSR2 snow water equivalent dataset, ERA-Interim SWE dataset, Global Land Data Assimilation System (GLDAS) SWE
21 dataset, GlobSnow SWE dataset, and ERA5-land SWE dataset, respectively, and it has a higher spatial resolution. The RRM
22 SWE product production method does not rely too much on an independent snow water equivalent product, it makes full use
23 of the advantages of each snow water equivalent dataset, and it considers the altitude factor. The average MAE of RRM SWE
24 product at different altitude intervals is 0.24 and the average RMSE is 23.55 mm, this method has good stability, it is extremely



25 suitable for the production of snow datasets with large spatial scales, and it can be easily extended to the preparation of other
26 snow datasets. The RRM SWE product is expected to provide more accurate snow water equivalent data for the hydrological
27 model and climate model and provide data support for cryosphere change and climate change studies. The RRM SWE product
28 is available from the ‘A Big Earth Data Platform for Three Poles’ (<http://dx.doi.org/10.11888/Snow.tpc.271556>) (Li et al.,
29 2021).

30 **1 Introduction**

31 The IPCC (Intergovernmental Panel on Climate Change) AR6 (Sixth Assessment Report) notes that the Northern Hemisphere
32 spring snow cover has greatly reduced since 1950, and the feedback effect of the climate system caused by this reduction is
33 extremely large (Masson-Delmotte et al., 2021). In most land areas of the Northern Hemisphere, annual runoff is dominated
34 by snowmelt, and accurately estimating the impacts of such a large amount of snowmelt runoff on ecosystems and human
35 activities is of great significance (Barnett et al., 2005; Bintanja and Andry, 2017; Henderson et al., 2018). Whether through
36 hydrometeorological simulation or global change research, the estimation of energy budget and mass of snow is very difficult,
37 so a set of highly accurate, long time series snow cover datasets is urgently needed to drive hydrometeorological simulations
38 and land surface process models. Among them, snow water equivalent data play an irreplaceable role as an important parameter
39 of the land surface hydrological model and climate model.

40 At present, there are many forms of snow water equivalent data in the world. According to type, these data can be divided
41 into site observation snow water equivalent (SWE), remote sensing SWE, reanalysis SWE, data assimilation SWE and model
42 simulation SWE. The remote sensing SWEs are mainly AMSR-E (Kelly, 2009) and AMSR2 (Imaoka et al., 2010; Tedesco and
43 Jeyaratnam, 2019). The reanalysis SWE mainly includes ERA-Interim (Dee et al., 2011), MERRA2 (Gelaro et al., 2017),
44 MERRA land (Reichle et al., 2011), and ERA5-land (Muñoz Sabater, 2019; Balsamo et al., 2015). The data assimilation SWE
45 mainly includes GlobSnow (Luoju et al., 2021) and Global Land Data Assimilation System (GLDAS) (Rodell et al., 2004).
46 The site observation SWE mainly includes the GHCN dataset (Menne et al., 2016). However, the time ranges of AMSR-E and
47 AMSR-E2 SWE are only from 2003 to present, which is lacking in terms of time series. Similarly, the GlobSnow SWE dataset



48 is also seriously lacking in time series. Although the reanalysis SWE data have good spatial and temporal continuity and high
49 data integrity, their accuracy is poor, and its MAE is 0.65 (Snauffer et al., 2016). The snow water equivalent data from stations
50 and meteorological observations cannot meet the needs of hydrometeorological and climate change research. This is mainly
51 because SWE from stations is discontinuous in time series and severely missing. Further, hydrometeorological studies often
52 require spatiotemporally continuous grid data to be driven (Pan et al., 2003). There are great differences among remote sensing
53 SWE, reanalysis SWE data, data assimilation SWE and observation SWE. For remote sensing SWE, the spatio-temporal
54 characteristics of different passive microwave snow water equivalent data differ significantly due to differences in sensors or
55 retrieval algorithms (Mudryk et al., 2015a). For data assimilation SWE and reanalysis SWE data, they also tend to exhibit
56 different spatio-temporal characteristics due to differences in model design, driving data, assimilation methods, etc. (Vuyovich
57 et al., 2014). In summary, although there are a variety of snow water equivalent data in the world, the data quality is uncertain.

58 Previous studies have shown that all kinds of snow water equivalent data in the Northern Hemisphere have advantages and
59 disadvantages, and none of these data perform well in all aspects (Mortimer et al., 2020). An effective method is to fuse all
60 kinds of snow water equivalent data in time and space, integrate the advantages of all kinds of data, and then generate a
61 relatively complete snow water equivalent dataset. Many scholars have conducted in-depth studies on snow water equivalent
62 data fusion. The main fusion methods can be classified into the following categories: multiproduct direct average (Mudryk et
63 al., 2015b), linear regression (Snauffer et al., 2016), data assimilation (Pulliainen, 2006), “multiple” collocation (Pan et al.,
64 2015) and machine learning (Snauffer et al., 2018; Xiao et al., 2018; Wang et al., 2020). Studies have shown that even the
65 simplest multisource data average is more accurate than a single snow water equivalent product (Snauffer et al., 2018).
66 However, the simple multisource data average cannot highlight the advantages of high-precision data, and it is easily affected
67 by the weight ratio of low-precision data, which reduces the accuracy of fused data (Mudryk et al., 2015a). Although the linear
68 regression method can make good use of the actual observation data to correct the original data, it is easy to overfit and causes
69 the overall deviation (Snauffer et al., 2016). The “multiple” collocation method changes the size of the original SWE data
70 before fusion, which easily causes data errors. The data assimilation method is sensitive to the accuracy of input data, and it is
71 difficult to fuse multisource data (Pan et al., 2015). In recent years, machine learning methods have been widely used in data
72 fusion (Santi et al., 2021; Ntokas et al., 2021). Machine learning methods can not only integrate the advantages of multisource



73 data but also make full use of site observation data to train the sample data, which easily generates snow water equivalent data
74 products with large spatial scales and long time series (Broxton et al., 2019; Bair et al., 2018).

75 In summary, based on the existing snow water equivalent data products, combining a machine learning algorithm to fuse
76 multisource snow water equivalent data is an effective method to prepare snow water equivalent products with long time series
77 and large spatial scales and retain the advantages of single snow water equivalent data products. In this study, we integrated
78 multisource snow water equivalent data products of RRM SWE based on the ridge regression model of the machine learning
79 algorithm. We selected ERA-Interim SWE data, GLDAS SWE data, GlobSnow SWE data, AMSR-E/AMSR2 SWE data, and
80 ERA5-land SWE data with relatively complete time series as the original data for the production of RRM SWE product. The
81 missing parts of the ERA-Interim SWE data, AMSR-E/AMSR2 SWE data, and GlobSnow SWE data are filled by the spatial-
82 temporal interpolation method. The GHCN dataset (Menne et al., 2016) and Russian snow survey data (Bulygina et al., 2011)
83 are used as training sample data of "true snow water equivalent", and the effect of altitude on the algorithm is also considered.
84 Thus, we prepared a set of spatiotemporal seamless snow water equivalent datasets (RRM SWE) covering the Pan-Arctic
85 region from 1979 to 2019. The spatial coverage of the RRM SWE product covers all land regions north of 45° N.

86 **2 Data and methods**

87 **2.1 Research region**

88 The research region of the RRM SWE product is located in the land region north of 45° N (hereinafter referred to as the Pan-
89 Arctic region) (Fig. 1). This region consists of Asia, Europe, and North America. The land region covers Russia, the United
90 States, Canada, Denmark, Norway, Iceland, Sweden, and Finland. This region has a cold climate and a wide area of snow
91 cover.

92 **2.2 Grid snow water equivalent data description**

93 In this study, we utilize ERA-Interim SWE data (Dee et al., 2011), GLDAS SWE data (Rodell et al., 2004), GlobSnow SWE
94 data (Luoju et al., 2021), AMSR-E/AMSR2 SWE data (Tedesco and Jeyaratnam, 2019), and ERA5-land SWE data (Muñoz



95 Sabater, 2019) as the original input datasets for the fusion data (Table 1).

96 GlobSnow is a dataset of global snow cover and snow water equivalents for the Northern Hemisphere released by the
97 European Space Agency (ESA) (<http://www.globsnow.info/swe/>) (Luojus et al., 2021). The SWE products in this dataset
98 combine the Canadian Meteorological Center (CMC) daily snow depth analysis data (Walker et al., 2011), ground weather site
99 observation data, and satellite microwave radiometer data. We obtained the L3A_daily_SWE product of this dataset. The
100 temporal resolution of the L3A_daily_SWE product is daily, the spatial resolution is 0.25°, and the data format is NETCDF4.

101 ERA-Interim is the fourth generation reanalysis data of the European Centre for Medium-Range Weather Forecasts
102 (ECMWF) (Dee et al., 2011). The data provide a global assimilated numerical product of various surface and top atmospheric
103 parameters from January 1979 to present (<https://apps.ecmwf.int/datasets/data/interim-full-daily/levtype=sfc/>). We obtained
104 the snow water equivalent dataset with a daily temporal resolution, a spatial resolution of 0.25°, and NETCDF4 data format.
105 The spatial range of the data is the Pan-Arctic region north of 45°N.

106 The Advanced Microwave Scanning Radiometer-Earth Observing System (AMSR-E) is a microwave scanning radiometer
107 on the Aqua satellite of the National Aeronautics and Space Administration (NASA) Earth Observing System (EOS) (Tedesco
108 and Jeyaratnam, 2019). The AMSR-E provides a global daily snow water equivalent dataset from June 19, 2002, to October 3,
109 2011 (https://nsidc.org/data/ae_dysno). AMSR2 is a microwave scanning radiometer on the GCOM-W1 satellite launched by
110 the Japan Aerospace Exploration Agency (JAXA) in May 2012. AMSR2 provides a global snow water equivalent dataset from
111 July 2, 2012 to present (https://nsidc.org/data/AU_DySno/versions/1). The spatial resolution of the AMSR-E SWE and
112 AMSR2 SWE datasets is 25 km x 25 km, the temporal resolution is daily, and the data formats are HDF-EOS and HDF-EOS5,
113 respectively.

114 The GLDAS is a model used to describe global land information; it contains data, such as global rainfall, water evaporation,
115 surface runoff, underground runoff, soil moisture, surface snow cover distribution, temperature, and heat flow distribution
116 (Rodell et al., 2004). This assimilation system includes data with spatial resolutions of 1°×1° and 0.25°×0.25° and temporal
117 resolutions of 3 hours, 1 day and 1 month. The GLDAS data are available for download from the Goddard Earth Sciences Data
118 and Information Services Center (GES DISC). We obtain a snow water equivalent dataset with the daily temporal resolution,
119 0.25° spatial resolution, and NETCDF4 data format.



120 ERA5-land is a reanalysis dataset that provides the evolution of global land parameter data since 1981 (Muñoz Sabater,
121 2019). The dataset provides eight types of snow parameter data, including snow albedo, snow cover, snow depth, snowfall, the
122 temperature of the snow layer, snowmelt, snow density, and snow water equivalent. This dataset provides a global snow water
123 equivalent dataset with a spatial resolution of hourly, the temporal resolution of $0.1^\circ \times 0.1^\circ$, temporal coverage of January 1981
124 to present, and data formats of GRIB and NETCDF4.

125 To maintain consistency in the spatial and temporal resolutions of the fused data, we unified the ERA-Interim SWE data,
126 GLDAS SWE data, GlobSnow SWE data, AMSR-E/AMSR2 SWE data, and ERA5-land SWE data into a daily temporal
127 resolution, with a spatial resolution of 0.25° and geographic projection of North Pole Lambert Azimuthal Equal Area.

128 2.3 Ridge regression machine learning algorithm for preparing snow water equivalent

129 In this study, we utilize the ridge regression model of a machine learning algorithm to fuse ERA-Interim SWE data (Dee et al.,
130 2011), GLDAS SWE data (Rodell et al., 2004), GlobSnow SWE data (Luo et al., 2021), AMSR-E/AMSR2 SWE data
131 (Tedesco and Jeyaratnam, 2019), and ERA5-land SWE data (Muñoz Sabater, 2019) to generate a set of new snow water
132 equivalent dataset of RRM SWE. The target reference data in this study are the GHCN dataset and Russian snow survey data.

133 The ridge regression model is a biased estimates regression method for collinear data analysis (Friedman et al., 2010; Hoerl
134 and Kennard, 1970b, a). By abandoning the unbiasedness of the ordinary least squares, this algorithm can obtain the regression
135 method in which the regression coefficient is more practical and reliable at the cost of losing part of the information and
136 reducing the accuracy. This model has high fitting accuracy for ill-conditioned data. The advantage of this model is that it uses
137 simple, accurate, and easy to prepare snow water equivalent products with long time series and large spatial scales. The
138 principle equation of the ridge regression model is defined as follows:

$$139 \hat{\beta}^{ridge} = \underset{\beta}{\operatorname{argmin}} \left\{ \sum_{i=1}^N \left(y_i - \beta_0 - \sum_{j=1}^p x_{ij} \beta_j \right)^2 + \lambda \sum_{j=1}^p \beta_j^2 \right\}, \quad (1)$$

140 where $\hat{\beta}^{ridge}$ is the extremum solution function of ridge regression. p is the number of variables involved in training. x_i is
141 the predicted snow water equivalent, y_i is the observed snow water equivalent, and λ , β , β_j and β_0 are the parameters



142 to be solved. $1, \dots, N$ is the sample of the training dataset. $\lambda \sum_{j=1}^p \beta_j^2$ is the penalty function terms. The model is developed in
143 python3, and the model framework is based on the "scikit-learn" machine learning library ([https://scikit-](https://scikit-learn.org/stable/index.html)
144 [learn.org/stable/index.html](https://scikit-learn.org/stable/index.html)), and the code is available.

145 The integration process of the RRM SWE product (Fig. 2) is described as follows:

- 146 1) The original ERA-Interim SWE data, GLDAS SWE data, GlobSnow SWE data, AMSR-E/AMSR2 SWE data, ERA5-
147 land SWE data, digital elevation model (DEM) data, unified temporal resolution, spatial resolution, projection, spatial
148 range, and unit are preprocessed.
- 149 2) The spatiotemporal interpolation method is used to fill in the missing data of AMSR-E/AMSR2 SWE, ERA-Interim SWE,
150 and GlobSnow SWE in space and time. Based on this method, the missing data of AMSR-E/AMSR2 SWE at low latitudes
151 and the missing data of ERA-Interim SWE and GlobSnow SWE on time series are filled.
- 152 3) The snow water equivalent data observed at stations from 1979 to 2014 are used as sample training data, and the AMSR-
153 E/AMSR2 SWE, ERA-Interim SWE, GLDAS SWE, GlobSnow SWE, ERA5-land SWE data, and DEM data are input
154 into the ridge regression model of a machine learning algorithm for training. During the model training process, we
155 restructured the training data, reduced the training data appropriately for the regions with denser training data, and make
156 it close to the amount of training data in the sparse region.
- 157 4) When the model was trained, ERA-Interim SWE, GLDAS SWE, GlobSnow SWE, and ERA5-land SWE were used for
158 training data between 1979 and 2002 (AMSR-E/AMSR2 SWE data were not available before 2002.), and AMSR-
159 E/AMSR2 SWE, ERA-Interim SWE, GLDAS SWE, GlobSnow SWE, and ERA5-land SWE were used for training data
160 after 2002.
- 161 5) Based on the S-Fold Cross Validation method, the snow water equivalent data are continuously trained and validated,
162 and finally select the optimal model and parameters are evaluated by the loss function.
- 163 6) Based on the trained optimal model, multiple snow water equivalent data products are integrated into the time series,
164 missing data are predicted, and a set of spatiotemporally seamless snow water equivalent datasets is generated.



165 7) Snow water equivalent data observed at stations from 2015 to 2019 are used to evaluate the accuracy of the RRM SWE
166 product.

167 **2.4 Site data and evaluation metrics**

168 **2.4.1 Site snow water equivalent data for training, validation, and testing**

169 Russian snow survey data (<http://aisori.meteo.ru/ClimateR>) include the average snow depth data and the average snow density
170 data of the station, and the snow water equivalent is the product of the measured average snow depth and the average snow
171 density (Bulygina et al., 2011). We obtained the snow water equivalent data of 19493 stations in 1979-2016 from this dataset.

172 GHCN-Daily is a comprehensive dataset that records the historical temperature, precipitation, and snow cover of the global
173 land area (Menne et al., 2016). This dataset is from the National Oceanic and Atmospheric Administration (NOAA)
174 (ftp://ftp.ncdc.noaa.gov/pub/data/ghcn/daily/by_year/). The dataset provides data from 75000 observation sites in 179
175 countries around the world. This dataset contains more than 40 meteorological elements, such as temperature, precipitation,
176 snow depth, snow water equivalent, wind speed, and evaporation capacity. We obtained data from all sites containing snow
177 water equivalents from 1979 to 2020.

178 We carefully screened the Russian snow survey data and GHCN data and eliminated some abnormal observation data to
179 ensure the high quality of the train set, validation set, and test set. The null values, negative numbers, and extreme snow water
180 equivalent value greater than 2000 mm are removed during the GHCN data screening process. The null values, negative
181 numbers, and extreme snow water equivalent value greater than 2000 mm are removed during the Russian snow survey data
182 screening process.

183 **2.4.2 Accuracy evaluation method for datasets**

184 Mean absolute error (MAE), root mean square error (RMSE), Pearson's correlation coefficient (R), and coefficient of
185 determination (R^2) are used to evaluate the accuracies of AMSR-E/AMSR2 SWE, ERA-Interim SWE, GLDAS SWE,
186 GlobSnow SWE, ERA5-land SWE, and the RRM SWE product. The specific equation of accuracy evaluation error is described
187 as follows.



188
$$MAE = \frac{1}{n} \sum_{i=1}^n |f_i - y_i|, \quad (2)$$

189
$$RMSE = \left[\frac{\sum_{i=1}^n (f_i - y_i)^2}{n} \right]^{\frac{1}{2}}, \quad (3)$$

190
$$R = \frac{1}{n-1} \sum_{i=1}^n \left(\frac{f_i - \bar{f}}{\sigma_f} \right) \left(\frac{y_i - \bar{y}}{\sigma_y} \right), \quad (4)$$

191
$$R^2 = \frac{\sum_{i=1}^n (f_i - \bar{f})^2}{\sum_{i=1}^n (y_i - \bar{y})^2}, \quad (5)$$

192 where n is the sample of the validation dataset, f_i is the snow water equivalent dataset product, and y_i is the measured snow
193 water equivalent at the station. \bar{f} and \bar{y} are the averages of snow water equivalent products and measured snow water
194 equivalents, respectively. σ_f and σ_y are the standard deviation of snow water equivalent products and measured snow water
195 equivalents, respectively.

196 To further evaluate the accuracy of the RRM SWE dataset at the spatial scale, we compared it with AMSR-E/AMSR2 SWE,
197 ERA-Interim SWE, GLDAS SWE, GlobSnow SWE, and ERA5-Land SWE at different altitude gradients. We also evaluate
198 MAE, RMSE, R and R^2 separately for 11 elevation intervals: <100 m, 100-200 m, 200-300 m, 300-400 m, 400-500 m, 500-
199 600 m, 600-700 m, 700-800 m, 800-900 m, 900-1000 m, and >1000 m.

200 We use the Mann-Kendall trend test (Mann, 1945; Kendall, 1990) method to evaluate the variation trend in the RRM SWE
201 dataset from 1979 to 2019 and analyze its reliability in terms of time series. Since the AMSR-E/AMSR2 SWE product and the
202 GlobSnow SWE product lacks snow water equivalent data for Greenland, we removed Greenland data to maintain consistency
203 in the spatial extent of the comparison data.



204 **3 Results and discussion**

205 **3.1 Overall accuracy evaluation of the RRM SWE product**

206 In this study, the accuracy of the RRM SWE, AMSR-E/AMSR2 SWE, ERA-Interim SWE, GLDAS SWE, GlobSnow SWE,
207 and ERA5-land SWE was compared using test datasets from 2015 to 2019. MAE, RMSE, R, and R^2 were used to reflect the
208 data quality of each snow water equivalent product.

209 According to the verification results in Fig. 3 and Table 2, the RRM SWE data have the best overall accuracy, and the MAE,
210 RMSE, R, and R^2 between the observed snow water equivalents are 0.24, 30.29 mm, 0.87, and 0.76, respectively. The overall
211 accuracy of the GlobSnow SWE and ERA5-land SWE products is higher than that of other snow water equivalent products.
212 The overall deviation of the GlobSnow SWE products is the smallest except for the RRM SWE data, with MAE and RMSE
213 values of 0.31 and 35.21 mm, respectively. Although the overall deviation between the GlobSnow SWE dataset and the
214 measured snow water equivalent is small, its correlation with the measured value is lower than that of the ERA5-land SWE
215 dataset, and it is missing data in terms of time series. The correlation between ERA5-land SWE and observed snow water
216 equivalent is the highest except for the RRM SWE data, with R and R^2 values of 0.84 and 0.70, respectively. The overall
217 deviation between the ERA5-land SWE dataset and the measured snow water equivalent is higher than that of the GlobSnow
218 SWE dataset, but its correlation with the measured values was higher than that of the GlobSnow SWE dataset, and its integrity
219 is better in terms of temporal and spatial series. In addition, the overall accuracy of the ERA-Interim SWE dataset and GLDAS
220 SWE dataset is relatively low, but their integrities are higher than that of the GlobSnow SWE dataset and AMSR-E/AMSR2
221 SWE dataset in terms of temporal and spatial series. The AMSR-E/AMSR2 SWE dataset has a higher estimation accuracy for
222 the low-value region of snow water equivalent. Moreover, in the Pan-Arctic region, most of the existing snow water equivalent
223 data products are missing to varying temporal and spatial degrees. Obviously, the accuracies of the existing snow water
224 equivalent products were uneven, and any kind of snow water equivalent dataset is not absolutely perfect.

225 The verification results also indicate the following ranking orders:

226 The MAE ranking order is RRM SWE < GlobSnow SWE < ERA5-land SWE < AMSR-E/AMSR2 SWE < ERA-Interim
227 SWE < GLDAS SWE.



228 The RMSE ranking order is RRM SWE < GlobSnow SWE < ERA5-land SWE < AMSR-E/AMSR2 SWE < ERA-Interim
229 SWE < GLDAS SWE.

230 The R ranking order is RRM SWE > ERA5-land SWE > GlobSnow SWE > ERA-Interim SWE > AMSR-E/AMSR2 SWE >
231 GLDAS SWE.

232 The R² ranking order is RRM SWE > ERA5-land SWE > GlobSnow SWE > ERA-Interim SWE > AMSR-E/AMSR2 SWE >
233 GLDAS SWE.

234 Compared with AMSR-E/AMSR2 SWE, ERA-Interim SWE, GLDAS SWE, GlobSnow SWE, and ERA5-land SWE, the
235 MAE of the RRM SWE and observed snow water equivalent is reduced by 0.23, 0.24, 0.32, 0.07, and 0.09, respectively. The
236 RMSE of the RRM SWE and observed snow water equivalent is reduced by 17.22 mm, 21.69 mm, 32.54 mm, 4.91 mm, and
237 7.82 mm, respectively. The correlation coefficient of the RRM SWE and observed snow water equivalent is improved by 0.30,
238 0.24, 0.45, 0.11, and 0.02, respectively. The coefficient of determination of the RRM SWE and observed snow water equivalent
239 is improved by 0.45, 0.37, 0.59, 0.20, and 0.06, respectively. Based on the above verification results, the accuracy of the RRM
240 SWE is significantly improved; the RRM SWE dataset has higher accuracy than any single grid snow water equivalent dataset,
241 and it also fills the gap in the original snow water equivalent data in terms of spatial and temporal resolutions.

242 Based on the kernel density estimation method, we analyze the density distribution of different SWE datasets (Fig. 4). The
243 results show that the RRM SWE dataset is closer to the 1:1 line and has the highest accuracy. The RRM SWE dataset is
244 particularly accurate for SWE estimation in the low-value region, and the test data are concentrated near the 1:1 line in the
245 high-density region (kernel density estimation > 0.00015) (Fig. 4). In contrast, the high-density regions of the GLDAS SWE
246 dataset, ERA-Interim SWE dataset, and AMSR-E/AMSR2 SWE dataset deviate significantly from the 1:1 line, resulting in
247 poor accuracy. The AMSR-E/AMSR2 SWE, GLDAS SWE, and GlobSnow SWE are underestimated relative to the snow water
248 equivalent measured at the site, among which GLDAS SWE underestimated the observed snow water equivalent the most
249 seriously, while ERA5-land SWE overestimated the observed snow water equivalent. Although the accuracies of GlobSnow
250 SWE and ERA5-land SWE are relatively high, their dispersion degrees are large (the kernel density estimation for most test
251 data is less than 0.0001). Overall, the RRM SWE data have a higher overall estimation accuracy, especially for the low-value
252 area of snow water equivalent.



253 However, in this study, there are still some uncertainties in the ridge regression machine learning model that integrates snow
254 water equivalent products. First, this model is strongly dependent on on-site observation data, and the fusion precision of snow
255 water equivalent is poor in some areas with sparse observation stations. The fusion accuracy of snow water equivalent products
256 will be affected to a certain extent without considering the prior snow cover information. Then, an underestimation of high
257 SWE remains in the RRM SWE product. The main reason is that there are few high SWE data in GHCN data and Russian
258 snow survey data, and the model lacks training samples with high SWE, which eventually leads to the underestimation of high
259 SWE by the machine learning model. Finally, in complex terrain, the integration of snow water equivalent products remains
260 challenging.

261 **3.2 Accuracy evaluation of the RRM SWE product at different altitudes**

262 The accuracy of each snow water equivalent product is not absolute at different altitude gradients based on evaluations of the
263 AMSR-E/AMSR2 SWE, ERA-Interim SWE, GLDAS SWE, GlobSnow SWE, and ERA5-land SWE products' accuracies (Fig.
264 5). The accuracy of a single snow water equivalent product is different from its overall accuracy. We consider the influence of
265 altitude in the algorithm and make full use of the accuracy advantage of each snow water equivalent data for different altitude
266 gradients.

267 The above verification results show that the MAEs between the RRM SWE dataset and measured snow water equivalent
268 are 0.19, 0.23, 0.27, 0.26, 0.25, 0.21, 0.26, 0.21, 0.32, 0.31, and 0.21, the RMSEs are 6 mm, 26 mm, 32 mm, 30 mm, 30 mm,
269 16 mm, 11 mm, 7 mm, 33 mm, 32 mm, and 35 mm, the R values are 0.97, 0.87, 0.86, 0.81, 0.82, 0.96, 0.86, 0.81, 0.88, 0.79,
270 and 0.81, and the R^2 values are 0.94, 0.75, 0.74, 0.65, 0.68, 0.91, 0.74, 0.65, 0.78, 0.62, and 0.66 at altitude gradients of <100
271 m, 100-200 m, 200-300 m, 300-400 m, 400-500 m, 500-600 m, 600-700 m, 700-800 m, 800-900 m, 900-1000 m and >1000
272 m, respectively (Fig. 5). Overall, RRM SWE product have the highest accuracy in the elevation interval <100 m, 100-200 m,
273 200-300 m, 400-500 m, 500-600 m, 600-700 m, 700-800 m, 800-900 m, and >1000 m. For the RRM SWE product itself, it
274 has the best performance in the elevation interval <100 m. The ERA5-land product has the best performance in the elevation
275 interval 300-400 m. The GlobSnow product has the best performance in the elevation interval 900-1000 m.



276 **3.3 Comparison of spatial distribution patterns between the RRM SWE product and traditional snow water equivalent** 277 **products**

278 A comparison of the annual average snow water equivalent distributions is made between the RRM SWE and AMSR-
279 E/AMSR2 SWE, ERA-Interim SWE, GLDAS SWE, GlobSnow SWE, and ERA5-land SWE in 2014, 2015, 2016, and 2017,
280 and their spatial distribution patterns are shown in Fig. 6.

281 Overall, the RRM SWE dataset, AMSR-E/AMSR2 SWE dataset, ERA-Interim SWE dataset, GLDAS SWE dataset,
282 GlobSnow SWE dataset, and ERA5-land SWE dataset have similar spatial distribution patterns in the Pan-Arctic region,
283 showing a trend of lower snow water equivalent in low latitudes and higher snow water equivalent in high latitudes. The
284 AMSR-E/AMSR2 SWE dataset covers a limited extent in the Pan-Arctic region, many data are missing, and low snow water
285 equivalent values at low latitudes. In northern Siberia, the ERA-Interim SWE product has a higher snow water equivalent, and
286 there are many abnormal, extreme snow water equivalent values ($SWE > 500$ mm) in this dataset. In low latitude regions,
287 Alaska, North Siberia, and the easternmost region of Russia, the snow water equivalent of GLDAS SWE products is
288 significantly lower. The GlobSnow SWE product lacks snow water equivalent data for Greenland, and this dataset has low
289 snow water equivalents in the Baffin Island, the Koryak Mountains, the Kamchatka Peninsula, and Alaska regions. The ERA5-
290 land SWE products have low snow water equivalents in northeastern Russia, Scandinavia, and northeastern Canada. The RRM
291 SWE dataset is more reasonable for estimating the spatial distribution of snow water equivalent in the Pan-Arctic, and the data
292 integrity is higher. Moreover, based on the new machine learning model, a variety of snow water equivalent data products in
293 different time series are fused, which makes the RRM SWE dataset completely temporally and spatially continuous.

294 The relative difference between the RRM SWE data and GLDAS SWE data is the highest, and the relative difference is
295 greater than 80% in most low altitude regions (Fig. 7). The relative difference between the RRM SWE data and the GlobSnow
296 SWE data is relatively small overall, especially in most high latitude areas where the relative difference is less than 10% (Fig.
297 7). Overall, the annual average relative differences of the RRM SWE data and AMSR2 SWE, ERA-Interim SWE, GLDAS
298 SWE, GlobSnow SWE, and ERA5-land SWE are 39%, 41%, 49%, 26%, and 33%, respectively (Fig. 7). Previous studies have
299 shown that the accuracy of snow water equivalent in the Northern Hemisphere estimated by GlobSnow SWE data is higher
300 (Pulliainen et al., 2020), while the spatial distribution pattern of the RRM SWE data is close to the estimation result of



301 GlobSnow SWE. In addition, the single point verification results based on the measured snow water equivalent data of
302 meteorological stations in section 4.1 show that the RRM SWE dataset has higher accuracy than the GlobSnow SWE dataset.
303 The RRM SWE dataset has good accuracy.

304 **3.4 Comparison of the annual variation tendencies of AMSR-E/AMSR2 SWE, ERA-Interim SWE, GLDAS SWE,**
305 **GlobSnow SWE, and ERA5-land SWE and the RRM SWE in the Pan-Arctic region**

306 Based on the Mann-Kendall trend test, we analyzed the changing trend in the annual average snow water equivalent of the
307 AMSR-E/AMSR2 SWE, ERA-Interim SWE, GLDAS SWE, GlobSnow SWE, ERA5-land SWE, and RRM SWE in the Pan-
308 Arctic region from 1979 to 2019.

309 Based on the Mann-Kendall trend test (see Fig. 8 and Table 3), from 1979 to 2019, the test value of the ERA-Interim annual
310 average snow water equivalent is 1.08, and there is no significant change trend under the significance test level of 0.05. The
311 test value of the GLDAS annual average snow water equivalent was 4.95 and showed a significant increasing trend at the
312 significance test level of 0.05. The test values of the AMSR-E/AMSR2 annual average SWE, GlobSnow annual average SWE,
313 ERA5-land annual average SWE, and RRM annual average SWE are -3.26, -2.54, -3.43, and -2.95, respectively, and these
314 four SWEs showed a significantly decreasing trend at the significance test level of 0.05. Based on the analysis of the RRM
315 SWE product, between 1979 and 2019, the annual average snow water equivalent in the Pan-Arctic decreased by 15.1 percent.
316 In the Northern Hemisphere, spring snow cover extent has decreased significantly, according to the Fifth Assessment Report
317 (AR5) of the IPCC. Between 1967 and 2010, the spring snow cover extent decreased by an average of 1.6 percent per decade,
318 while the June snow cover extent decreased by 11.7 percent per decade (Stocker, 2014). Most studies have shown that the
319 annual variation tendency of snow depth and snow cover extent showed a significant decreasing trend in the Northern
320 Hemisphere (Brutel-Vuilmet et al., 2013), which is consistent with the annual variation tendency of the RRM SWE dataset.
321 This dataset can reflect the characteristics of snow cover change in the Pan-Arctic under the background of climate change
322 and can be used as the driving data for the climate model to support climate change-related research. In addition, this dataset
323 is expected to provide a snow data basis for the study of "Arctic amplification".



324 **4 Data availability**

325 The RRM SWE product is available for free download from the ‘A Big Earth Data Platform for Three Poles’
326 (<http://dx.doi.org/10.11888/Snow.tpd.271556>) (Li et al., 2021). The temporal resolution of RRM SWE product is daily, and
327 the spatial resolution is 10 km. It spans latitude 45°N-90°N and longitude 180°W-180°E. A brief summary and data description
328 document (includes data details, spatial range, usage method and etc.) are also provided.

329 **5 Conclusions**

330 In this study, we propose a method to fuse multisource snow water equivalent data by a ridge regression model based on
331 machine learning. A new method was utilized to prepare a set of spatiotemporal seamless snow water equivalent datasets of
332 RRM SWE, combined with the original AMSR-E/AMSR2 SWE dataset, ERA-Interim SWE dataset, GLDAS SWE dataset,
333 GlobSnow SWE dataset, and ERA5-land SWE dataset. In the RRM SWE dataset, the time series of the data is 1979-2019, the
334 temporal resolution is daily, the spatial resolution is 10 km, and the spatial range is the Pan-Arctic region.

335 The RRM SWE data product has the best accuracy, especially for the estimation of low snow water equivalent. The accuracy
336 ranking of the snow water equivalent dataset verified by the test dataset is described as follows: RRM SWE > GlobSnow
337 SWE > ERA5-land SWE > AMSR-E/AMSR2 SWE > ERA-Interim SWE > GLDAS SWE. The accuracy of the RRM SWE
338 dataset is higher than that of the existing snow water equivalent products at most elevation intervals. Moreover, the RRM SWE
339 dataset fills in the missing data of the original snow water equivalent dataset spatiotemporally.

340 Compared with traditional fusion methods, machine learning methods have a good advantage. We find that the simple
341 machine learning algorithm not only has high efficiency but also has good accuracy in the preparation of snow water equivalent
342 products on a global scale. Without losing the advantages of existing snow water equivalent products, this method can also
343 make full use of station observation data to integrate the advantages of various snow water equivalent products. The model
344 training process does not rely too much on a specific sample, and this model has a strong generalization ability. In addition,
345 the influence of altitude on the preparation scheme is considered in detail in the model. Compared with the snow water
346 equivalent dataset prepared by the traditional method, the spatial resolution is only 25 km, while this new method obtains a



347 snow water equivalent dataset with a higher spatial resolution of 10 km.

348 We propose that the RRM SWE dataset preparation scheme has good continuity and can prepare real-time and high-quality
349 snow water equivalent datasets in the Pan-Arctic. In addition, the new method proposed in this paper has the advantages of
350 simplicity and high precision in preparing large-scale snow water equivalent datasets and can be easily extended to the
351 preparation of other snow datasets. This dataset is an important supplement to the Pan-Arctic snow water equivalent database
352 and is expected to provide data support for Arctic cryosphere studies and global climate change studies.

353 **Author contribution.**

354 DS and HL designed the study and wrote the manuscript; JW, XH, and TC contributed to the discussions, edits, and revisions.
355 DS and WJ compiled the model code.

356 **Competing interests.**

357 The authors declare that they have no conflict of interest.

358 **Acknowledgements.**

359 The authors would like to thank the European Space Agency (ESA) for GlobSnow data, the European Centre for Medium-
360 Range Weather Forecasts (ECMWF) for ERA-Interim data and ERA5-land data, the National Aeronautics and Space
361 Administration (NASA) for AMSR-E/AMSR2 data, the Goddard Earth Sciences Data and Information Services Center (GES
362 DISC) for GLDAS data, the Russian Federal Service For Hydrometeorology and Environmental Monitoring
363 (ROSHYDROMET) for snow survey data, and the National Oceanic and Atmospheric Administration (NOAA) for GHCN-
364 Daily SWE data.



365 **Financial support.**

366 This research was supported by the Strategic Priority Research Program of the Chinese Academy of Sciences (Grant No.
367 XDA19070302), the National Science Fund for Distinguished Young Scholars (Grant No. 42125604), the National Natural
368 Science Foundation of China (Grant No. 41971399, 41971325, 42171391).

369 **References**

370 Bair, E. H., Abreu Calfa, A., Rittger, K., and Dozier, J.: Using machine learning for real-time estimates of snow water
371 equivalent in the watersheds of Afghanistan, *The Cryosphere*, 12, 1579-1594, 2018.

372 Balsamo, G., Albergel, C., Beljaars, A., Boussetta, S., Brun, E., Cloke, H., Dee, D., Dutra, E., Munoz-Sabater, J., Pappenberger,
373 F., de Rosnay, P., Stockdale, T., and Vitart, F.: ERA-Interim/Land: a global land surface reanalysis data set, *Hydrol Earth Syst*
374 *Sc*, 19, 389-407, 10.5194/hess-19-389-2015, 2015.

375 Barnett, T. P., Adam, J. C., and Lettenmaier, D. P.: Potential impacts of a warming climate on water availability in snow-
376 dominated regions, *Nature*, 438, 303-309, 10.1038/nature04141, 2005.

377 Bintanja, R. and Andry, O.: Towards a rain-dominated Arctic, *Nat Clim Change*, 7, 263-+, 10.1038/Nclimate3240, 2017.

378 Broxton, P. D., Van Leeuwen, W. J., and Biederman, J. A.: Improving snow water equivalent maps with machine learning of
379 snow survey and lidar measurements, *Water Resources Research*, 55, 3739-3757, 2019.

380 Brutel-Vuilmet, C., Menegoz, M., and Krinner, G.: An analysis of present and future seasonal Northern Hemisphere land snow
381 cover simulated by CMIP5 coupled climate models, *Cryosphere*, 7, 67-80, 10.5194/tc-7-67-2013, 2013.

382 Bulygina, O. N., Groisman, P. Y., Razuvaev, V. N., and Korshunova, N. N.: Changes in snow cover characteristics over
383 Northern Eurasia since 1966, *Environmental Research Letters*, 6, Artn 045204
384 10.1088/1748-9326/6/4/045204, 2011.

385 Dee, D. P., Uppala, S. M., Simmons, A., Berrisford, P., Poli, P., Kobayashi, S., Andrae, U., Balmaseda, M., Balsamo, G., and
386 Bauer, d. P.: The ERA-Interim reanalysis: Configuration and performance of the data assimilation system, *Quarterly Journal*
387 *of the royal meteorological society*, 137, 553-597, 2011.



- 388 Friedman, J., Hastie, T., and Tibshirani, R.: Regularization Paths for Generalized Linear Models via Coordinate Descent, *J Stat*
389 *Softw*, 33, 1-22, DOI 10.18637/jss.v033.i01, 2010.
- 390 Gelaro, R., McCarty, W., Suarez, M. J., Todling, R., Molod, A., Takacs, L., Randles, C. A., Darmenov, A., Bosilovich, M. G.,
391 Reichle, R., Wargan, K., Coy, L., Cullather, R., Draper, C., Akella, S., Buchard, V., Conaty, A., da Silva, A. M., Gu, W., Kim,
392 G. K., Koster, R., Lucchesi, R., Merkova, D., Nielsen, J. E., Partyka, G., Pawson, S., Putman, W., Rienecker, M., Schubert, S.
393 D., Sienkiewicz, M., and Zhao, B.: The Modern-Era Retrospective Analysis for Research and Applications, Version 2
394 (MERRA-2), *J Climate*, 30, 5419-5454, 10.1175/Jcli-D-16-0758.1, 2017.
- 395 Henderson, G. R., Peings, Y., Furtado, J. C., and Kushner, P. J.: Snow-atmosphere coupling in the Northern Hemisphere, *Nat*
396 *Clim Change*, 8, 954-+, 10.1038/s41558-018-0295-6, 2018.
- 397 Hoerl, A. E. and Kennard, R. W.: Ridge regression: applications to nonorthogonal problems, *Technometrics*, 12, 69-82, 1970a.
398 Hoerl, A. E. and Kennard, R. W.: Ridge regression: Biased estimation for nonorthogonal problems, *Technometrics*, 12, 55-67,
399 1970b.
- 400 Imaoka, K., Kachi, M., Fujii, H., Murakami, H., Hori, M., Ono, A., Igarashi, T., Nakagawa, K., Oki, T., Honda, Y., and Shimoda,
401 H.: Global Change Observation Mission (GCOM) for Monitoring Carbon, Water Cycles, and Climate Change, *P Ieee*, 98, 717-
402 734, 10.1109/Jproc.2009.2036869, 2010.
- 403 IPCC, 2021: Climate Change 2021: The Physical Science Basis. Contribution of Working Group I to the Sixth Assessment
404 Report of the Intergovernmental Panel on Climate Change [Masson-Delmotte, V., P. Zhai, A. Pirani, S.L. Connors, C. Péan, S.
405 Berger, N. Caud, Y. Chen, L. Goldfarb, M.I. Gomis, M. Huang, K. Leitzell, E. Lonnoy, J.B.R. Matthews, T.K. Maycock, T.
406 Waterfield, O. Yelekçi, R. Yu, and B. Zhou (eds.)]. Cambridge University Press. In Press.
- 407 Kelly, R.: The AMSR-E Snow Depth Algorithm: Description and Initial Results, 2009.
- 408 Kendall, M. G.: Rank Correlation Methods, *British Journal of Psychology*, 25, 86-91, 1990.
- 409 Li, H., Shao, D., Li, H., Wang, W., Ma, Y., and Lei, H.: Arctic Snow Water Equivalent Grid Dataset (1979-2019), A Big Earth
410 Data Platform for Three Poles [dataset], 10.11888/Snow.tpd.271556, 2021.
- 411 Luoju, K., Pulliainen, J., Takala, M., Lemmetyinen, J., Mortimer, C., Derksen, C., Mudryk, L., Moisander, M., Hiltunen, M.,
412 and Smolander, T.: GlobSnow v3. 0 Northern Hemisphere snow water equivalent dataset, *Scientific Data*, 8, 1-16, 2021.



- 413 Mann, H. B.: Nonparametric test against trend, *Econometrica*, 13, 245-259, 1945.
- 414 Menne, M., Durre, I., Korzeniewski, B., McNeal, S., Thomas, K., Yin, X., Anthony, S., Ray, R., Vose, R., and Gleason, B.:
415 Global Historical Climatology Network–Daily (GHCN-Daily), Version, 3, V5D21VHZ, 2016.
- 416 Mortimer, C., Mudryk, L., Derksen, C., Luoju, K., Brown, R., Kelly, R., and Tedesco, M.: Evaluation of long-term Northern
417 Hemisphere snow water equivalent products, *The Cryosphere*, 14, 1579-1594, 2020.
- 418 Mudryk, L., Derksen, C., Kushner, P., and Brown, R.: Characterization of Northern Hemisphere snow water equivalent datasets,
419 1981–2010, *Journal of Climate*, 28, 8037-8051, 2015a.
- 420 Mudryk, L. R., Derksen, C., Kushner, P. J., and Brown, R.: Characterization of Northern Hemisphere Snow Water Equivalent
421 Datasets, 1981-2010, *J Climate*, 28, 8037-8051, 10.1175/Jcli-D-15-0229.1, 2015b.
- 422 Muñoz Sabater, J.: ERA5-Land hourly data from 1981 to present, Copernicus Climate Change Service (C3S) Climate Data
423 Store (CDS), 2019.
- 424 Ntokas, K. F., Odry, J., Boucher, M.-A., and Garnaud, C.: Investigating ANN architectures and training to estimate snow water
425 equivalent from snow depth, *Hydrology and Earth System Sciences*, 25, 3017-3040, 2021.
- 426 Pan, M., Fisher, C. K., Chaney, N. W., Zhan, W., Crow, W. T., Aires, F., Entekhabi, D., and Wood, E. F.: Triple collocation:
427 Beyond three estimates and separation of structural/non-structural errors, *Remote Sens Environ*, 171, 299-310,
428 10.1016/j.rse.2015.10.028, 2015.
- 429 Pan, M., Sheffield, J., Wood, E. F., Mitchell, K. E., Houser, P. R., Schaake, J. C., Robock, A., Lohmann, D., Cosgrove, B., and
430 Duan, Q.: Snow process modeling in the North American Land Data Assimilation System (NLDAS): 2. Evaluation of model
431 simulated snow water equivalent, *Journal of Geophysical Research: Atmospheres*, 108, 2003.
- 432 Pulliainen, J.: Mapping of snow water equivalent and snow depth in boreal and sub-arctic zones by assimilating space-borne
433 microwave radiometer data and ground-based observations, *Remote Sens Environ*, 101, 257-269, 10.1016/j.rse.2006.01.002,
434 2006.
- 435 Pulliainen, J., Luoju, K., Derksen, C., Mudryk, L., Lemmetyinen, J., Salminen, M., Ikonen, J., Takala, M., Cohen, J.,
436 Smolander, T., and Norberg, J.: Patterns and trends of Northern Hemisphere snow mass from 1980 to 2018 (vol 41, pg 861,
437 2020), *Nature*, 10.1038/s41586-020-2416-4, 2020.



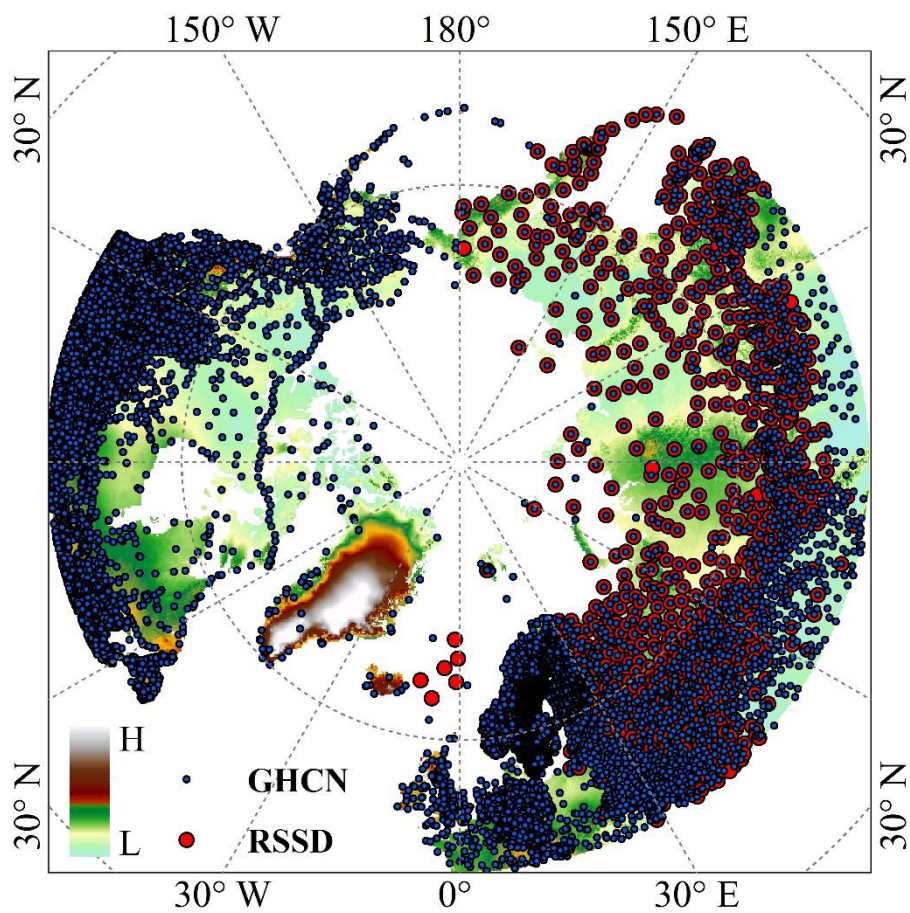
- 438 Reichle, R. H., Koster, R. D., De Lannoy, G. J. M., Forman, B. A., Liu, Q., Mahanama, S. P. P., and Toure, A.: Assessment and
439 Enhancement of MERRA Land Surface Hydrology Estimates, *J Climate*, 24, 6322-6338, 10.1175/Jcli-D-10-05033.1, 2011.
- 440 Rodell, M., Houser, P., Jambor, U., Gottschalck, J., Mitchell, K., Meng, C.-J., Arsenault, K., Cosgrove, B., Radakovich, J., and
441 Bosilovich, M.: The global land data assimilation system, *Bulletin of the American Meteorological Society*, 85, 381-394, 2004.
- 442 Santi, E., Brogioni, M., Leduc-Leballeur, M., Macelloni, G., Montomoli, F., Pampaloni, P., Lemmetyinen, J., Cohen, J., Rott,
443 H., and Nagler, T.: Exploiting the ANN Potential in Estimating Snow Depth and Snow Water Equivalent From the Airborne
444 SnowSAR Data at X-and Ku-Bands, *IEEE Transactions on Geoscience and Remote Sensing*, 2021.
- 445 Snauffer, A. M., Hsieh, W. W., and Cannon, A. J.: Comparison of gridded snow water equivalent products with in situ
446 measurements in British Columbia, Canada, *Journal of Hydrology*, 541, 714-726, 2016.
- 447 Snauffer, A. M., Hsieh, W. W., Cannon, A. J., and Schnorbus, M. A.: Improving gridded snow water equivalent products in
448 British Columbia, Canada: multi-source data fusion by neural network models, *Cryosphere*, 12, 891-905, 10.5194/tc-12-891-
449 2018, 2018.
- 450 Stocker, T.: *Climate change 2013: the physical science basis: Working Group I contribution to the Fifth assessment report of*
451 *the Intergovernmental Panel on Climate Change*, Cambridge university press 2014.
- 452 Tedesco, M. and Jeyaratnam, J.: AMSR-E/AMSR2 Unified L3 Global Daily 25 km EASE-Grid Snow Water Equivalent,
453 Version 1.[online] Boulder, Colorado USA, NASA National Snow and Ice Data Center Distributed Active Archive Center,
454 2019.
- 455 Vuyovich, C. M., Jacobs, J. M., and Daly, S. F.: Comparison of passive microwave and modeled estimates of total watershed
456 SWE in the continental U nited S tates, *Water resources research*, 50, 9088-9102, 2014.
- 457 Walker, A., Brasnett, B., and Brown, R.: Canadian Meteorological Centre (CMC) daily gridded snow depth analysis for
458 Northern Hemisphere, 1998-2008, 2011.
- 459 Wang, J. W., Yuan, Q. Q., Shen, H. F., Liu, T. T., Li, T. W., Yue, L. W., Shi, X. G., and Zhang, L. P.: Estimating snow depth by
460 combining satellite data and ground-based observations over Alaska: A deep learning approach, *J Hydrol*, 585, ARTN 124828
461 10.1016/j.jhydrol.2020.124828, 2020.
- 462 Xiao, X. X., Zhang, T. J., Zhong, X. Y., Shao, W. W., and Li, X. D.: Support vector regression snow-depth retrieval algorithm



463 using passive microwave remote sensing data, Remote Sens Environ, 210, 48-64, 10.1016/j.rse.2018.03.008, 2018.

464

465



466

467 **Figure 1: The DEM and snow survey stations of the research region (GHCN is the Global Historical Climatology Network station,**

468 **and RSSD is the Russian snow survey station).**

469

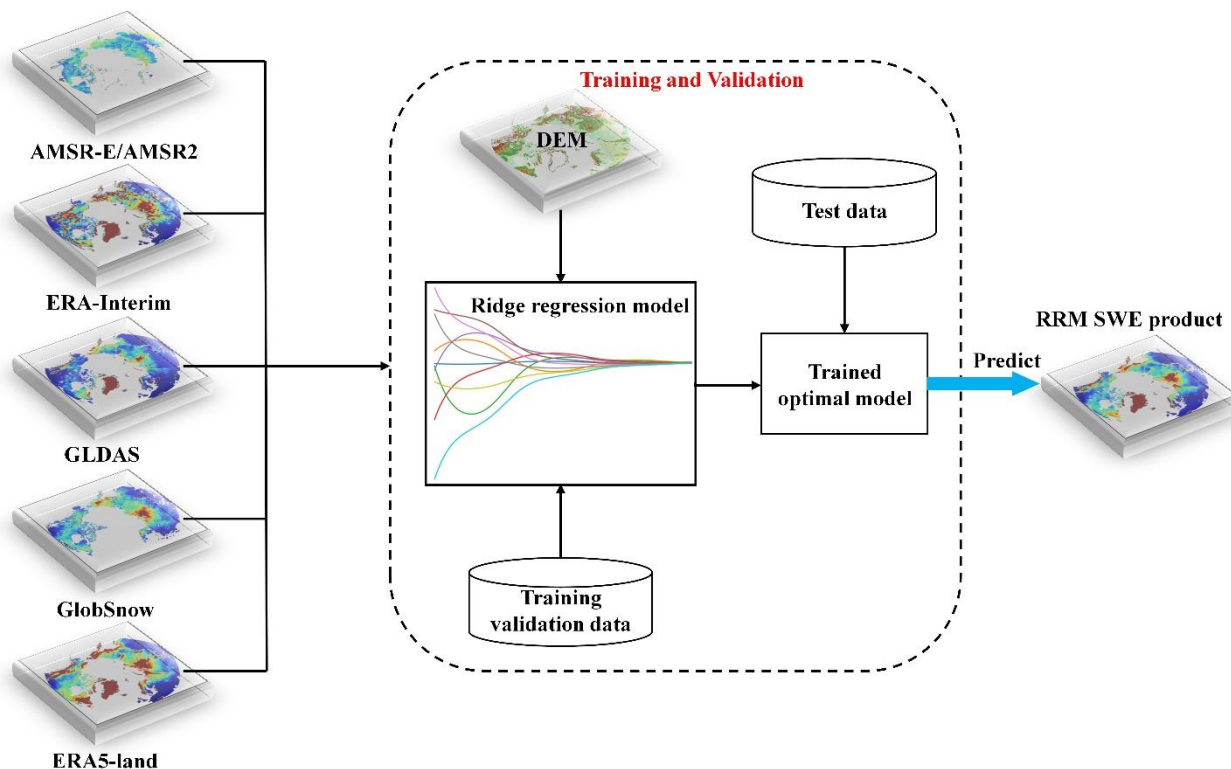
470



471 **Table 1: Introduction to the SWE data.**

Data type	Data name	Time series	Temporal resolution	Spatial resolution	Spatial coverage	File format
Remote sensing data	AMSR-E/AMSR2	2002-2011/2012-2020	Daily	25 km x 25 km	Global (No Greenland)	HDF5
Data assimilation dataset	GLDAS	1979-2020	Daily	0.25°×0.25°	Global	NetCDF
	GlobSnow	1979-2018	Daily	0.25°×0.25°	Northern Hemisphere (No Greenland)	NetCDF
Reanalysis dataset	ERA-Interim	1979-2019	Daily	0.25°×0.25°	Global	NetCDF
	ERA5-land	1981- present	Hour	0.1°×0.1°	Global	NetCDF

472
 473
 474



475

476 **Figure 2: Flow chart of RRM SWE data preparation (preparation of spatiotemporal seamless snow water equivalent datasets mainly**

477 **includes three processes: model training, model reasoning, and snow water equivalent data preparation).**

478

479

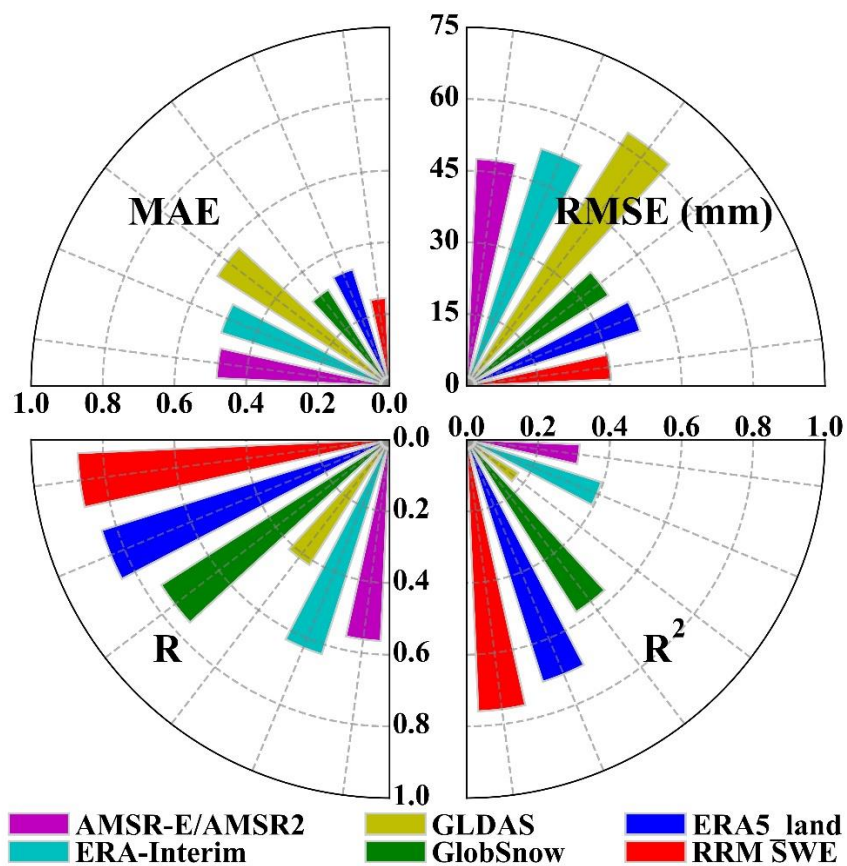


480 **Table 2: Error list for the station data and grid snow water equivalent products.**

Error type	MAE	RMSE (mm)	R	R ²
ERA-Interim	0.49	51.98	0.62	0.39
AMSR-E/AMSR2	0.48	47.51	0.56	0.31
GLDAS	0.56	62.84	0.41	0.17
GlobSnow	0.31	35.21	0.75	0.56
ERA5-land	0.34	38.11	0.84	0.70
RRM SWE	0.24	30.29	0.87	0.76

481

482



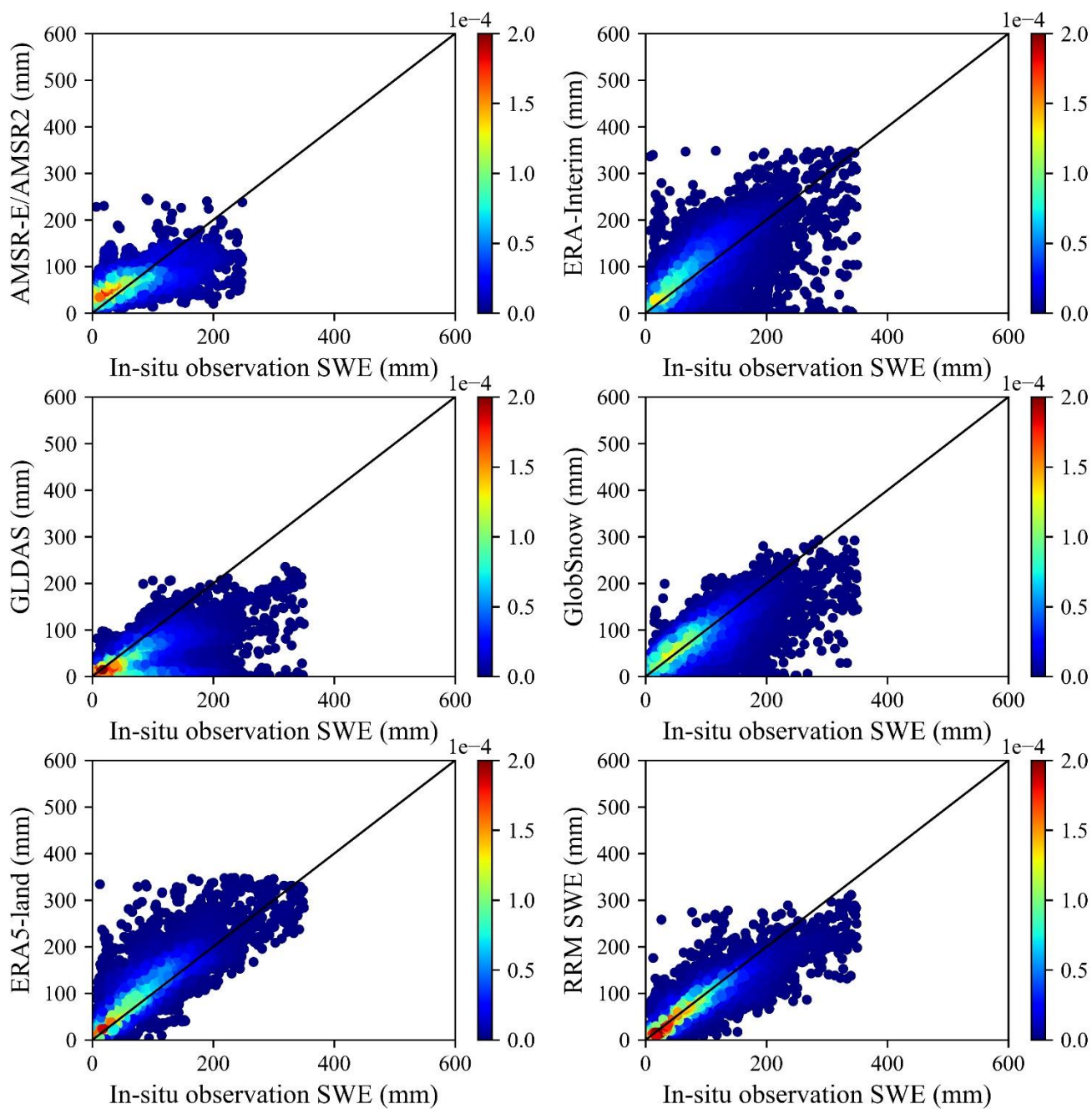
483

484

485

486

Figure 3: Accuracy comparison of various snow water equivalent products. The upper left sector represents MAE, the upper right sector represents RMSE, the lower-left sector represents R, and the lower right sector represents R^2 . The sector axis represents the size of the error, and the color represents different snow water equivalent datasets.



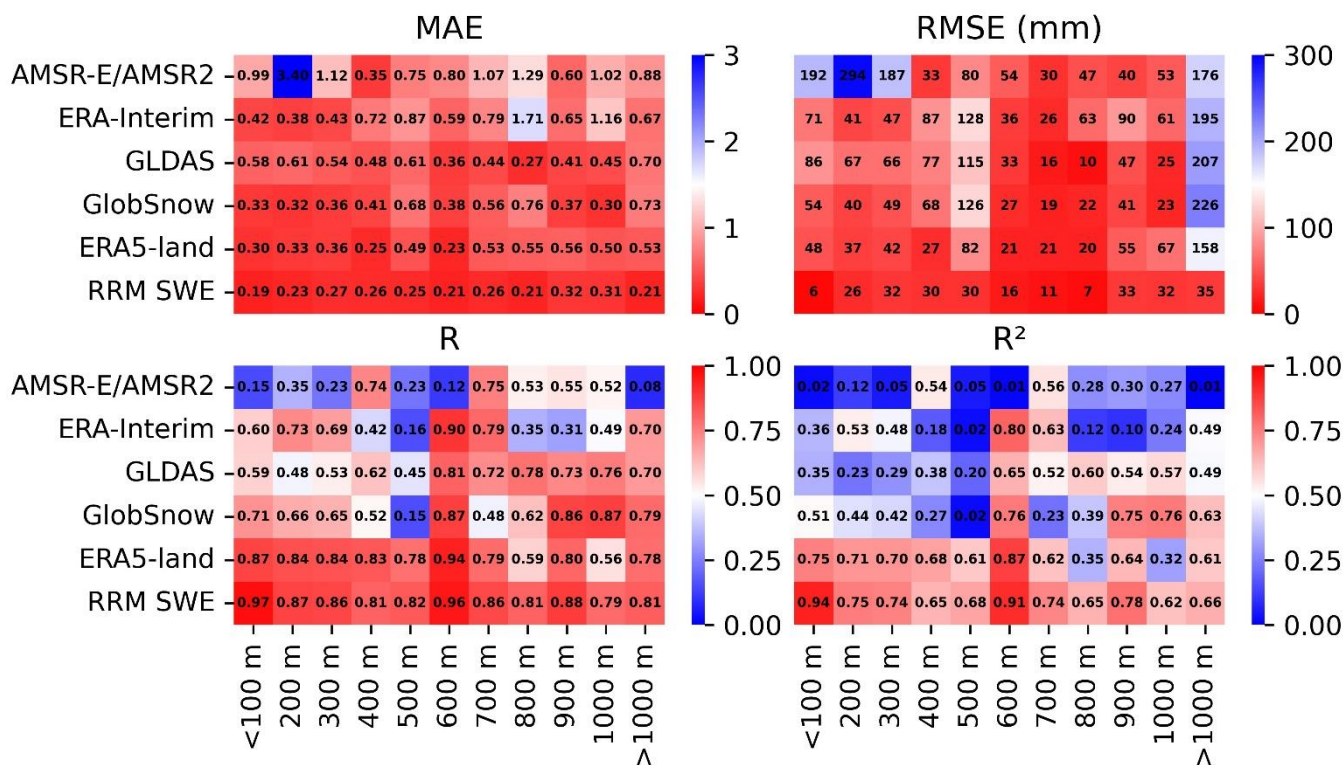
487

488

489

490

Figure 4: Error verification density diagram (A total of 8618 sample points were used for verification.). The color bar represents the value of kernel density estimation. The closer the high-density area is to the 1:1 line, the higher the verification accuracy of the dataset is at most of the measuring stations.



491

492

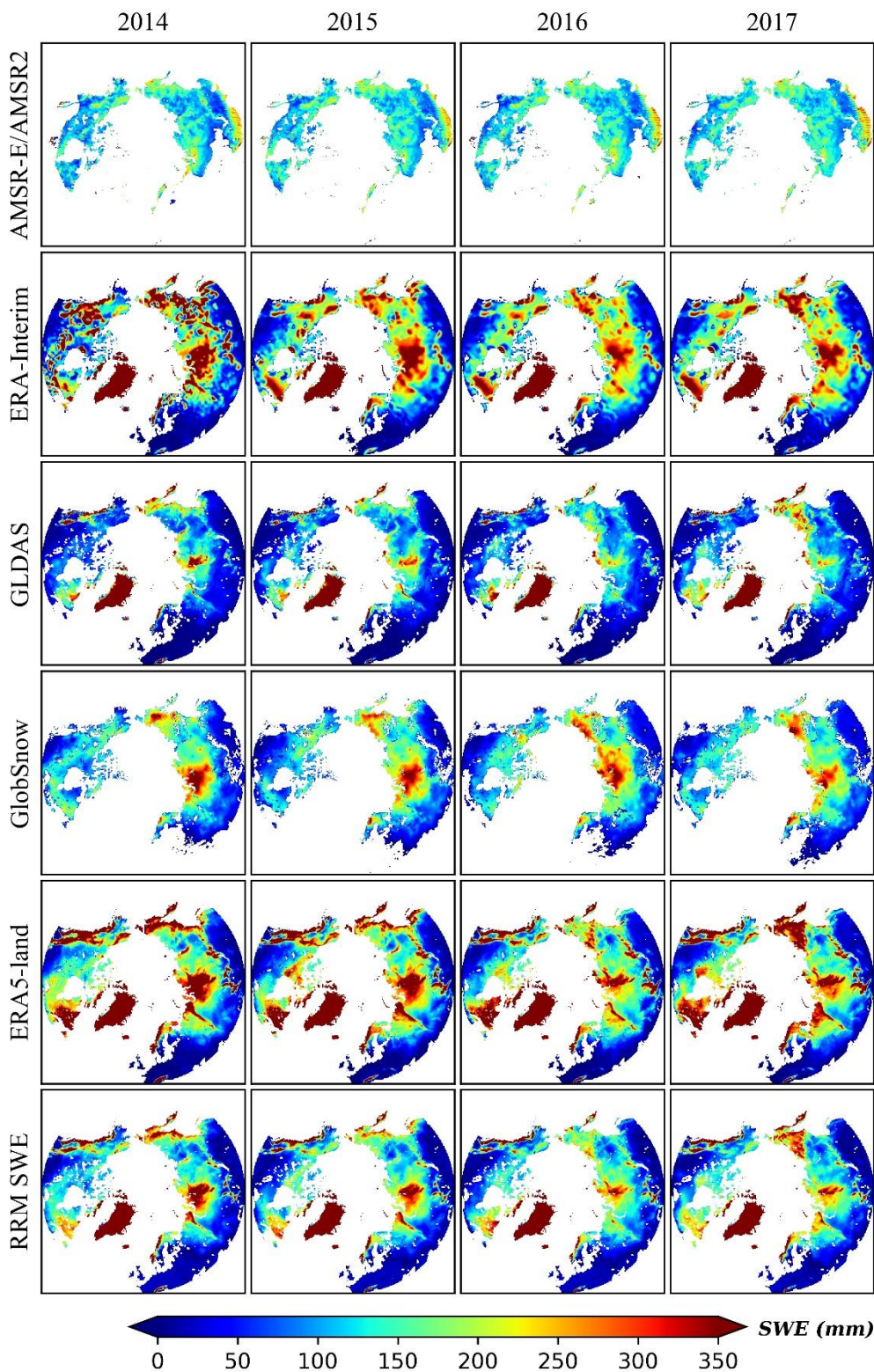
493

494

495

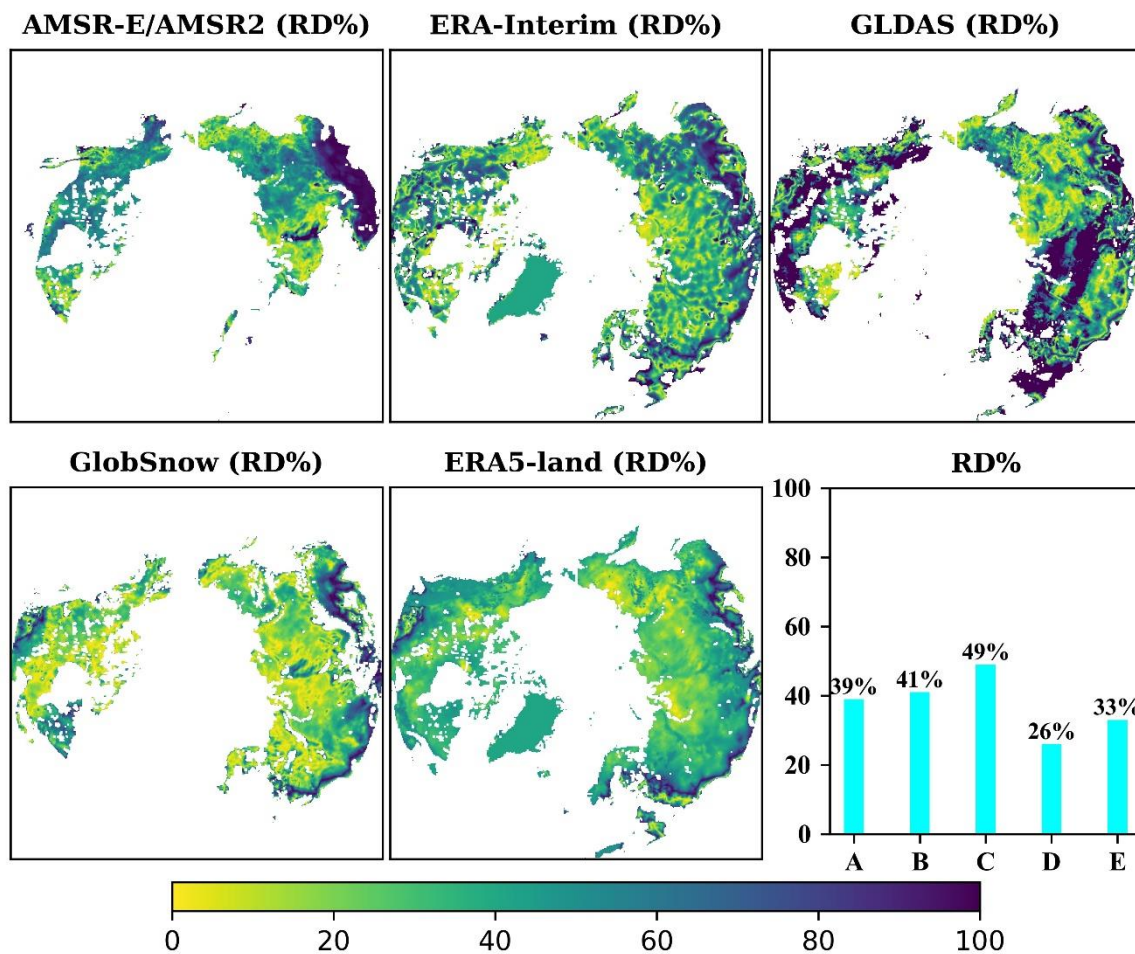
496

Figure 5: Comparison of the error between the RRM SWE and AMSR-E/AMSR2 SWE, ERA-Interim SWE, GLDAS SWE, GlobSnow SWE, and ERA5-land SWE at different altitudes (the abscissa represents the altitude gradient, and the ordinate represents different snow water equivalent datasets). The color bar indicates the error in each snow water equivalent dataset. The closer to red the color is, the higher the accuracy is. MAE: mean absolute error, RMSE: root mean square error, R: Pearson's correlation coefficient, R²: coefficient of determination).



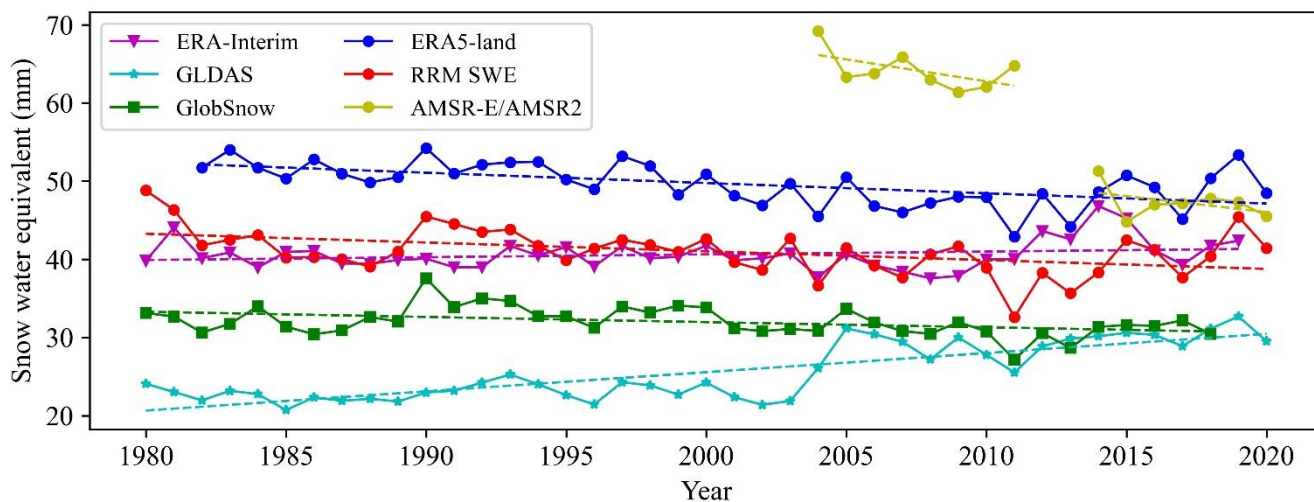


498 **Figure 6: Comparison of the spatial distribution characteristics between the RRM SWE and AMSR-E/AMSR2 SWE, ERA-Interim**
499 **SWE, GLDAS SWE, GlobSnow SWE, and ERA5-land SWE (the four columns of images represent the comparison results in 2014,**
500 **2015, 2016, and 2017, respectively).**
501



502

503 **Figure 7: Temporal and spatial distributions of relative differences (RD%) between the RRM SWE and AMSR-E/AMSR2 SWE,**
504 **ERA-Interim SWE, GLDAS SWE, GlobSnow SWE, and ERA5-land SWE. Lower right subgraph: Comparison of annual average**
505 **relative differences between the RRM SWE and AMSR2 SWE (A), ERA-Interim SWE (B), GLDAS SWE (C), GlobSnow SWE (D),**
506 **and ERA5-land SWE (E).**



507

508 **Figure 8: Annual variation tendency in the AMSR-E/AMSR2 SWE, ERA-Interim SWE, GLDAS SWE, GlobSnow SWE, and ERA5-**
509 **land SWE and RRM SWE products from 1979 to 2019 (the dotted line is the trend line calculated based on the Mann-Kendall**
510 **method).**

511



512 **Table 3: Results of the Mann-Kendall trend test performed for various snow water equivalent products for 1979 to 2019.**

Data	P-value	Test value	Trend
AMSR-E/AMSR2	0.00	-3.26	Decreasing
ERA-Interim	0.27	1.08	No trend
GLDAS	7.29e-07	4.95	Increasing
GlobSnow	0.01	-2.54	Decreasing
ERA5-land	0.00	-3.43	Decreasing
RRM SWE	0.00	-2.95	Decreasing

513 *Significance level $\alpha = 0.05$